Karnatak University Journal of Science 55(3), (2024), 1–11

Karnatak University Journal of Science

ISSN: 0075-5168

ORIGINAL ARTICLE

Green Synthesized Zero-Dimensional Carbon Dots Modified Glassy Carbon Electrode for the Enhanced Sensing of Genestein

Ranjita D Tandel[1], **J Seetharamappa**[1,*]

[1] *Department of Chemistry, Karnatak University, Dharwad, 580 003, Karnataka, India*

ARTICLE INFO

Article history:
Received 29.01.2024
Accepted 26.08.2024
Published 27.09.2024

[*] *Corresponding author.*
J Seetharamappa
jseetharam97@gmail.com

https://doi.org/10.61649/kujos/v55i3.24.2

ABSTRACT

The present study explores carbon dots (CDs) modified glassy carbon electrode (GCE) for the sensing of a flavonoid, genestein (GEN). CDs were prepared by hydrothermal reaction involving the heating of EDTA at 150 °C for 4 h. The proposed CDs modified GCE (CDs/GCE) was used to investigate the electrochemical behaviour of GEN by CV. The voltammetric measurements were conducted in phosphate buffer solution (PBS) of pH 3. Under optimized conditions a linear relationship between peak current and concentration of GEN was noticed in the range of 0.5-30.01, 0.1-54.16 and 1.0-62.5 μM for differential pulse voltammetric (DPV), square wave voltammetric (SWV) and adsorptive stripping differential pulse voltammetric (AdSDPV), respectively. The applicability of the proposed methods was demonstrated by analyzing spiked human urine samples and the results were found to be satisfactory. In addition, the proposed sensor was successfully used to understand the mechanism of binding between GEN and bovine serum albumin.

Keywords: Genestein; Carbon dots; Electrochemical methods; Analytical applications

1 INTRODUCTION

Isoflavones are a group of phytochemicals, used to prevent and treat chronic diseases. Isoflavones represent a subgroup of flavonoids commonly found in peanuts, soybeans and chick pea [1]. In particular, genestein (GEN) is a predominant dietary isoflavone aglycone having a 3-phenylchromone skeleton and is present in legumes such as soy and its products. They are naturally occurring chemical constituent that may interact with estrogen receptors to produce weak estrogenic or anti-estrogenic effects. It has been reported to exhibit many health benefits such as osteoporosis, cardiovascular disease, and post-menopause symptoms. It has received much attention due to its potential anticarinogenic, antioxidative, antiproliferative and antibacterial effects [2–4]. As a result of the above pharmacological effects, different kinds of herbal preparations that contain GEN as active component has been used clinically as therapeutical agent. Therefore, establishment of sensitive and selective analytical tool for the determination of GEN in clinical, pharmaceuticals and food samples assume importance. Some analytical methods are reported for the determination of GEN, including HPLC [5, 6], capillary zone electrophoresis [7], UV-vis spectrophotometry [8] etc. Although these methods have advantages of sensitivity and accuracy, their complicated operations and cost of the instrument limit their application. Electroanalytical techniques have advantages over other analytical methods such as higher sensitivity, low detection limits, instrument simplicity, low cost, ease of use and rapid response. GEN is an electroactive species so it can be detected by electrochemical methods. Although electrochemical determination of GEN has been reported [5, 7, 9], detailed oxidation mechanism has not been fully characterized. So, the understanding of oxidation behaviour of GEN, as well as its analytical determination is of great relevance.

CDs have been acknowledged as discrete spherical particles with sizes less than 10 nm. They possess sp^2 conjugated core with suitable oxygen content in the form of carboxyl, aldehyde, and hydroxyl groups. Since the discovery of CDs in 2004, much attention has been paid to produce luminescent materials because of their outstanding qualities such as chemical inertness, luminescence, excellent

biocompatibility, low cost, and potential applications [10–12]. CDs are fluorescent carbon nanostructure that could potentially replace metal based toxic quantum dots due to their benign, abundant, and inexpensive nature. In addition to low toxicity, CDs produce outstanding optical properties such as high resistance to photobleaching, high quantum yields and, symmetric and narrow emissions [13, 14]. Over the years, CDs have great potential applications in bioimaging, photoelectrochemistry, sensing, photoelectronics, electro-chemiluminescence and drug delivery. A number of top-down and bottom-up methods have been reported for the synthesis of CDs. Top-down methods including laser ablation [15], arc discharge method [16] and chemical reactions [17]. However, these methods involve non-selective exfoliation process and therefore may require special equipment. On the other hand, bottom-up approaches like carbonization of glucose, ascorbic acid, sucrose and citric acid etc have gained the significant attention for the production of fluorescent CDs [15, 18–21]. These methods avoid tedious pretreatment process and use of strong acids. The synthesis of CDs using environmentally friendly solvents and nontoxic chemicals is the key issue for green strategy. Although carbonization of citric acid, sucrose etc., has been explored for the synthesis of carbon dots, most of the reported process involves strong acids as well as post treatments with surface passivation [22–24]. The additional use of chemicals in the synthesis of hetero atom doped carbon dots increases the toxic risk from multi chemicals. Therefore, it is worthwhile to develop a one-pot green synthesis of fluorescent carbon dots for sensor applications.

Binding of small molecules to protein induces changes that deeply modify the binding and thermodynamic properties of the macromolecules and result in new and unexpected properties. Serum albumin is the major component of blood plasma [25, 26]. Bovine serum albumin (BSA) is a single chain 582 amino acids residue. It plays an important role in the transport and disposition of a variety of endogenous and exogenous ligands in blood. It has a wide range of physiological functions involving the binding, transport, and delivery of fatty acids. Binding of BSA to drugs makes an essential factor in studying drug-plasma interactions [27]. It gets more interested by considering the drug in blood is circulated in two probable forms. Only the free drugs interact with the receptor to produce beneficial effects. Since, the unbound drug concentration is proportional and depends on the plasma unbound drug, the study and evaluation of BSA- drugs interactions are found to be primary and important factor in understanding the pharmacological and pharmacokinetics effects of drugs [28–30].

The present study mainly describes the use of eco-friendly synthesized zero-dimensional CDs as electrochemical sensors to accelerate the electron transfer process between the sensing interface and electrode. Herein, we report an environmentally friendly one pot method to fabricate carbon dots modified GCE. CDs anchored well on the GCE surface. The proposed modified electrode exhibited high conductivity for GEN. Meanwhile, the proposed electrode was used to investigate the GEN-BSA interaction.

2 EXPERIMENT

2.1 Reagents and apparatus

Genestein, ascorbic acid and BSA were purchased from Sigma Aldrich and were used as received without further purification. A stock solution of 1 mM GEN was prepared by dissolving an appropriate amount of GEN in ethanol and stored refrigerator at 4 °C when not using. Phosphate buffer solutions of different pH ranging from 3.0-10.0 were used as supporting electrolyte. All other chemicals and reagent used were of analytical grade.

The structure morphologies of CDs were characterized by transmission electron microscope (TEM) Philips (CM200) and powder X-ray diffraction analysis was done on X-ray diffraction system (Bruker AXS D8) employing the Cu K_α line (1.5406 Å). Surface morphology of the prepared sensor was examined by using atomic scope microscopy (AFM). All electrochemical measurements were carried out with a conventional three electrode system. The modified glassy carbon electrode was used as working electrode. Ag/AgCl as reference electrode and platinum wire as a counter electrode. Cyclic voltammetry was recorded in phosphate buffer solution. Electrochemical impedance spectroscopic measurements were carried out on a CHI-6134E by applying an alternating current (AC) voltage with 5 mV amplitude in a frequency range from 0.1 Hz to 100 kHz. All the experiments were performed in room temperature.

2.2 Synthesis of CDs

Fluorescent CDs were prepared by hydrothermal method using EDTA as carbon source. Briefly, 0.2 g of EDTA was dissolved in 5 mL ultra-pure water with constant stirring. Then, the solution was transferred to 25 mL Teflon lined stainless steel autoclave. Further, the autoclave was heated to 150 °C in a furnace for 4 h. It was cooled to room temperature. The obtained dark brown product was centrifuged for 10 min to remove large size particles. The CDs suspension was prepared by dispersing 5 mg of CDs in 5 mL distilled water using ultrasonic agitation for 30 min. This stable suspension was used to modify the GCE. Finally, the suspension of CDs was stored and used for further applications.

2.3 Preparation of CDs modified GCE

The modified electrode was prepared by a simple casting method. Prior to the surface coating the GCE was carefully polished with 1.0 and 0.05 μm alumina powder, respectively and then rinsed with distilled water. In order to obtain modified electrode, an aliquot of 7 μL of CDs suspension was dropped on GCE surface. Then the electrode was dried under the IR lamp to give the target electrode of CDs/GCE.

3 RESULTS AND DISCUSSION

3.1 Characterization of CDs

XRD analysis was carried out to calculate particle size of carbon dots. XRD pattern of CDs showed partially crystalline nature of CDs with a broad peak at 43.28° which is attributed to (101) pattern of graphitic carbon (Figure 1 **A**). The peak around 26° shows an interlayer spacing of 3.6 Å which corresponds to (002) plane. Presence of peak around 25.3° attributed to highly ordered carbon in graphite CDs. This indicated the disorder nature of CDs, which in turn responsible for conductive properties of CDs. The interlayer spacing was calculated using the Bragg's equation shown below based on the position of reflection peaks:

$$n\lambda = 2d \sin\theta$$

where n is the positive integer 1, λ is the wavelength of incident light used (λ = 1.54 Å) and θ is the angle between the incident rays and the surface of the material. The calculated interlayer distance of around 0.38 nm matches well with the results obtained from TEM images. Further, average particle size of CDs was calculated by using Debye-Scherrer's equation, d = 0.9 λ/β cosθ, and was found to be in the order of 2.0 - 4.5 nm. These results revealed the successful formation of CDs. The functional groups on the surface of CDs were investigated by FTIR spectroscopy (Figure 1**B**). The band near 3400 cm^{-1} and the bands within the range of 1000-1300 cm^{-1} correspond to O-H bending vibrations and C-OH stretching. This confirmed the presence of –COOH groups on CDs. The bands around 1618 and 1764 cm^{-1} could be assigned for C=C and C=O stretching respectively. All these functional groups present around CDs confirmed the excellent hydrophillicity of CDs.

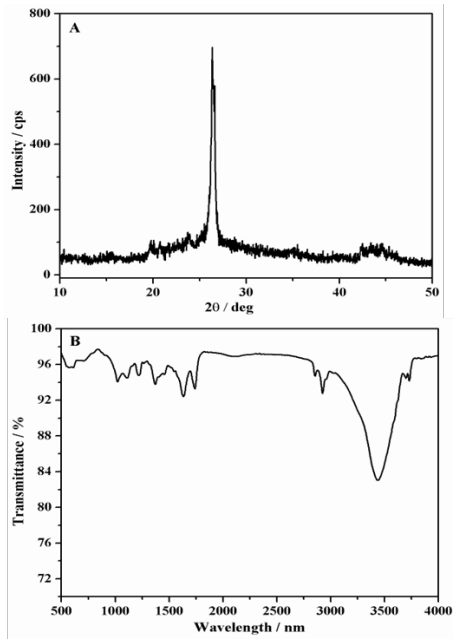

Figure 1: A) XRD pattern and B) FTIR spectrum of CDs

UV-vis absorption and fluorescence spectra of CDs were recorded to evaluate the optical properties. The absorption spectrum of CDs showed a peak in UV region around 345 nm that is characteristic of n→π* transition of C=O bond (Figure 2**A**). Raman spectrum is to detect the possible defects in the structure of carbonaceous materials caused by the presence of oxygenated functional groups. Raman spectrum of CDs is shown in Figure 2 **B**. The D band at 1329 cm^{-1} was attributed to the presence of disorder defects, while the G band at 1650 cm^{-1} was attributed to the vibrations of C=C bond. The ratio of intensity of D and G bands (ID/IG) is a measurement of the ratio of sp^3/sp^2 carbons and the extent of disorder property. The ratio of relative intensities of D and G bands for CDs was calculated to be 0.84 indicating the presence of oxygenated functional groups (C-O, C=O, O-C-O) that resulted in the creation of defects in the structure of CDs.

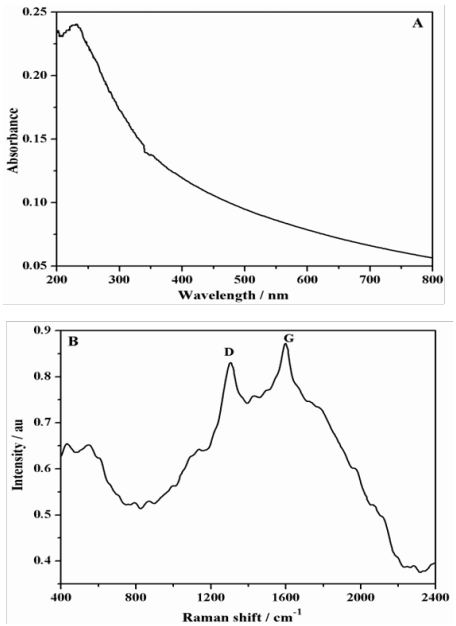

Figure 2: UV-visible absorption (A) and Raman (B) spectrum of CDs

Morphology of the prepared CDs was characterized by transmission electron microscopy (TEM). Figure 3**A** shows the TEM image of uniform CDs with an average diameter of ~4-5 nm. Corresponding enlarged TEM image shown in Figure 3 **B** indicated the crystalline structure of CDs. The lattice spacing was measured to be around 0.34 nm which is in agreement with the (102) facet of graphite.

The morphology and height profile of CDs was studied by atomic force microscopy. The sample for AFM studies was prepared by dropping aqueous dispersion of CDs on the mica substrate followed by drying under IR lamp. As shown in Figure 4**A & B**, AFM images revealed that the synthesized CDs have an average size distribution of ~5.2 nm. Further, fluorescence spectrum was recorded. Upon excitation at 360

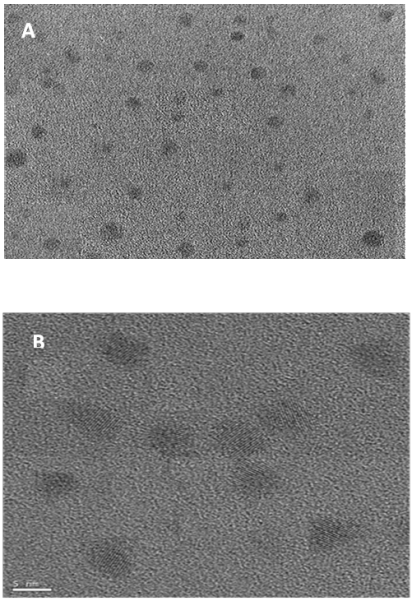

Figure 3: TEM images of CDs (A and B)

nm, maximum emission wavelength was noticed at 440 nm (Figure 4 **C**). Moreover, the emission wavelengths were red shifted with increase in wavelength indicating the presence of different sizes of CDs.

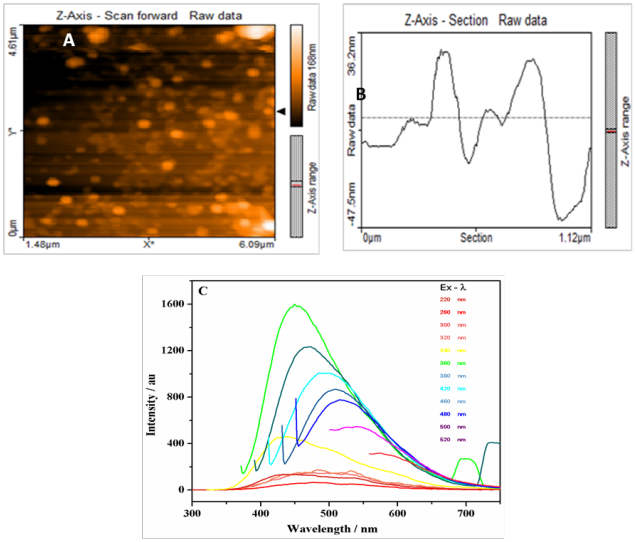

Figure 4: AFM micrographs of CDs (A and B) and C) Excitation-dependent emission spectra of CDs

3.2 Characterization of sensing interfaces by electrochemical and impedance techniques

Heterogeneous charge transfer kinetics of bare GCE and CDs/GCE were studied by cyclic voltammetric method using 1 mM $K_4[Fe(CN)_6]$ as a redox probe. Figure 5 **A** shows the cyclic voltammograms of 1 mM $K_4[Fe(CN_6)]$ in 0.1 M KCl at bare GCE and CDs/GCE with a scan rate of 0.1 V s^{-1}. A pair of well-defined redox peaks was noticed at bare GCE (~ 10.1 μA). Upon the modification of GC surface with CDs, the redox peak currents were observed to be increased (~ 61.4 μA). Moreover, the potential difference between the anodic and cathodic peaks (ΔE_p) of redox probe at CDs/GCE was about ~62 mV which is lesser than that at bare GCE (120 mV). The decrease in the value of ΔE_p indicated the increased electrode conductivity and significant catalytic performance of CDs/GCE. The increased peak current observed at CDs/GCE compared to that noticed at bare electrode was attributed to the increased electroactive surface area of modified electrode. The surface area of the electrode was calculated by cyclic voltammetry using Randles-Sevcik equation shown below:

$$I_p = 2.69 \times 10^5 n^{3/2} A C_0 D_R^{1/2} v^{1/2}$$

Where I_p refers to the peak current, n is the number of electrons taking part in the redox process, A is the surface area of the electrode (cm^2), D_R is the diffusion coefficient, C_0 is the concentration of $K_4[Fe(CN)_6]$ and ν is the scan rate. For 1 mM $K_4[Fe(CN)_6]$ in 0.1 M KCl electrolyte, n= 1 and $D_R = 7.6 \times 10^{-6}$ cm s^{-1}. The electroactive surface areas were calculated to be 0.051 cm^2 and 0.41 cm^2 for bare and CDs/GCE respectively. Thus, larger surface area of CDs/GCE facilitated the electron transfer rate.

It is well known that electrochemical impedance spectroscopy is the one of the powerful tools and non-destructive technique used to study the interface properties of the modified electrodes [31]. The Nyquist plot consist of real and imaginary part. A linear section at lower frequency is attributed to a diffusion-limited process and a semicircle portion observed at higher frequencies corresponds to the electron-transfer limited process. The value of the diameter of semicircle reflects the interfacial charge transfer resistance (R_{ct}). The R_{ct}, solution resistance (R_s), constant phase element (CPE) and surface heterogeneity (n) of the modified surface were obtained from the semicircle of the Nyquist plot. Impedance spectra of bare GCE and modified GCE were recorded in 0.1 M KCl containing 1 mM $K_4[Fe(CN)_6]^{3-/4-}$ as redox probe and the results are shown in Figure 5**B**. A semicircle domain with R_{ct} of 22.50 Ω was observed (curve a) in Figure 5 **B**. Upon the modification of GCE with CDs, the diameter of semicircle was noticed to be decreased indicating the presence of conductive material on the surface of GCE (R_{ct} = 8.37 Ω, curve b). Other parameters of equivalent circuits are given in Table 1. The roughness factor n was found to be close to unity at CDs/GCE. These results demonstrate that the electron transfer ability of CDs/GC electrode was enhanced due to the presence of CDs on GCE. The impedance results are in good agreement with cyclic voltammetric measurements.

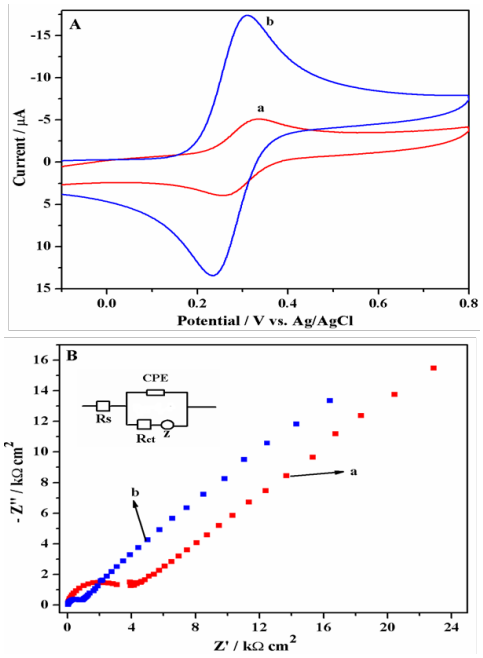

Figure 5: Cyclic voltammograms (A) and impedance spectra (B) of 1mM $[Fe(CN)_6]^{3-/4-}$ at bare GCE (a) and CDs/GCE (b) in 1.0 M KCl . Inset: Equivalent circuits for stepwise modified Bent-GO (B) and Bent-ErGO (C).of GOms-ErGO (c).

Table 1: Electrochemical characteristics of different modified electrodes

Modified GCE	Voltammetric results			Impedance spectroscopic results				
	Area cm^2	ΔE_p mV	I_p μA	R_{ct} Ω cm^2	R_s Ω cm^2	CPE μF cm^{-2}	n	W_0 kΩ cm^2
CDs	0.41	62	61.4	8.37	1.04	12.65	0.92	2.15X10^{-4}
Bare	0.051	120	10.1	22.50	1.13	9.03	0.81	1.41X10^{-4}

3.3 *Electrochemical studies of GEN at CDs/GCE and bare GCE*

In order to understand the use of CDs/GCE for electrochemical studies and for the assay of GEN, cyclic voltammograms of 10 μM GEN were recorded in phosphate buffer solution of pH 3 at bare and modified GCE at the scan rate of 0.1 V s^{-1}. As shown in Figure 6 **A**, during the first anodic sweep from 0 to 1.6 V, two oxidation peaks (E_{pa1} = 0.703 and E_{pa2} = 1.063 V) were observed at bare GCE corresponding to oxidation groups present in GEN moiety. No peak was observed during the cathodic scan indicating the irreversible behaviour of GEN molecule. Under identical conditions, the response of GEN was greatly enhanced (~ 30 fold) at GCE modified with CDs. Besides this, a shift in the peak potential (0.015 V) was also noticed. The negative shift in the oxidation peak potential and noticeable enhanced peak current revealed that the CDs exhibited catalytic activity in the oxidation of GEN. This was attributed to the presence of CDs which transferred the electron towards GEN at CDs modified GCE.

3.4 *Effect of pH*

Choosing the appropriate pH of supporting electrolyte is an important step in the investigation of electrochemical behaviour of bioactive molecules since the pH influences peak potential, peak current and shape of the voltammogram. Figure 6 **B** shows the cyclic voltammetric responses of 10 μM GEN in PBS of different pH (3.0 – 8.0) at CDs/GCE. GEN exhibited two anodic peaks at pH 3. However, its peak current and potential varied with raise in pH. In basic solution (beyond pH 8) no oxidation peak was observed. This could be attributed to the presence of repulsive force operating between the drug and electrode surface. This prevented the arrival of drug to electrode surface. The best results were achieved with PBS of pH 3 at 0.703 V. Hence, pH 3 was selected for further studies. The relationship between the peak potential and pH was also studied. It was found that the value of peak potential shifted to negative end with increase in pH revealing the involvement of protons in the electrode process. The relationship can be described by the equation, E_{p1} (V) = 0.052 pH + 0.869, R^2 = 0.968; E_{p2} (V) = 0.061 pH + 1.261, R^2 = 0.983. According to Nernst equation, the number of electrons and protons involved in the electro-oxidation was calculated approximately 1:1 based on the slope of 0.0592 V/pH. The slope of 0.052 V/pH and 0.061 V/pH were approximately close to the theoretical value of 0.0592 V/pH, suggesting that the electron transfer was accompanied by equal number of protons and electrons (1:1).

3.5 *Influence of scan rate*

To investigate the reaction mechanism, the effect of scan rate on cyclic voltammetric response of 10 μM GEN was examined at CDs/GCE in the range of 10-300 mV/s. As shown in Figure 7**A,** the oxidation peak current of GEN increased with increase in the scan rate while their oxidation peak potentials were shifted towards positive end. The plot of logarithms of peak currents versus logarithms of scan rates exhibited the linear relationship (Figure 7 **B**) and the corresponding regression equations are shown below:

$$\log i_{pa1} = 0.625 \log \upsilon - 4.471;\ R^2 = 0.995$$

$$\log i_{pa2} = 0.608 \log \upsilon - 4.567;\ R^2 = 0.996$$

According to literature [32], the slope of 0.5 in the log-log plot of indicates a diffusion-controlled electrode process. The electrode process was proposed to be diffusion controlled. In the present, since the slope values of 0.625 and 0.608 for peak a_1 and a_2 respectively, are close to 0.5. In order to calculate the number of protons and electrons in the electrode process, Laviron's equation shown below for an irreversible electrochemical process is used.

$$E_p = E^0 + (RT/\alpha nF) \ln (RTk_s/\alpha nF) + (RT/\alpha nF) \ln \upsilon$$

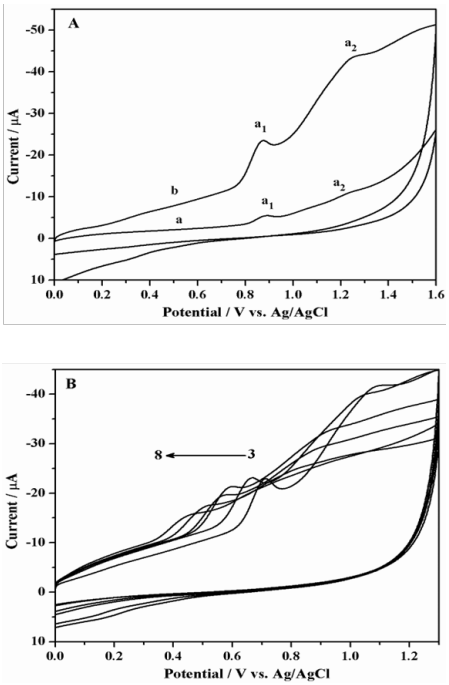

Figure 6: A): Cyclic voltammograms of 10 μM GEN at bare GCE (a), and C-dots/GCE (b) in phosphate buffer of pH 3 B) Cyclic voltammograms of 10 μM GEN at CDs/GCE in phosphate buffer of different pH (3 - 8)

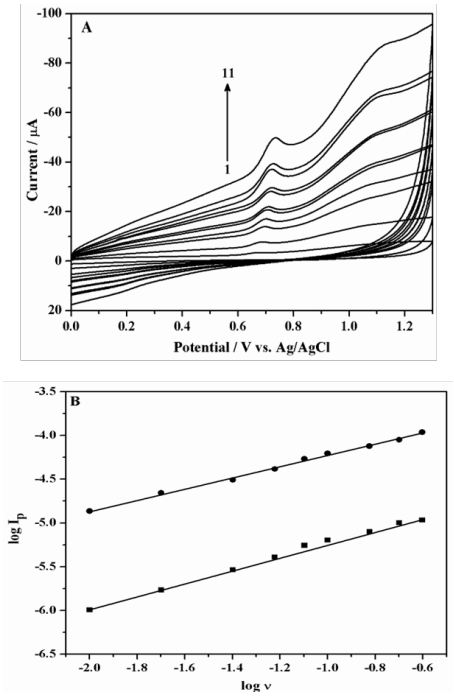

Figure 7: A) Cyclic voltammograms of 10 μM GEN on CDs/GCE at different scan rates (10 - 300 mVs^{-1}) in phosphate buffer of pH 3; B) Dependence of log I_p on log υ

where E^0 is the standard electrode potential, k_s is the heterogeneous rate constant, α is the charge transfer coefficient, which is generally considered to be 0.5, n is the number of electrons involved in the rate determining step and R, T, F and υ have their usual meanings. The value of αn can be calculated from the slope of E_p vs ln υ plot, and the relationship between E_p and lnυ could be expressed as E_{pa1} = 0.034x + 0.951, R^2 = 0.919 and E_{pa2} = 0.022x + 1.235, R^2 = 0.985 respectively. The values of slope were found to be 0.034 and 0.013. Thus, αn values were calculated to be 0.753 and 1.163 respectively for peak a_1 and a_2 respectively. The value of n and k_s were calculated to be 1.5 and 1.05 for peak a_1 and 2.3 and 1.10 s^{-1} for peak a_2 respectively. From these results, we propose that one and two electrons were involved in the oxidation process of GEN (Scheme 1).

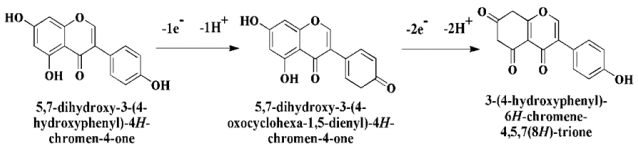

Scheme 1: **Mechanism of oxidation of GEN**

3.6 Optimization of electrochemical conditions

Optimization of parameters is an important stage in the development of an electro-analytical method, because these parameters influence the shape and peak height. Thus, the experimental conditions including the amount of CDs suspension and accumulation time were optimized. The peak currents of GEN increased significantly with increase in CDs volume (from 1 to 7 μL) and decreased rapidly beyond 7 μL (Figure 8 **A**). This is due to the formation of thicker film of CDs on GCE that blocked the electrode surface and so electron transfer occurred with difficulty between the electrode and analyte molecules. Therefore, only 7 μL of CDs suspension was chosen as the optimum volume to modify the GCE.

The influence of accumulation time on the electrochemical response of GEN is shown in Figure 8**B**. As can be seen from Figure 8 **B**, the peak current of GEN increased rapidly with increase in the accumulation time and reached maximum at 150 s, indicating that the adsorption equilibrium was reached beyond 150 s. Beyond 150 s, it decreased. The electrical conductivity was hindered by the prolonged electron transfer path created by the thicker covering of CDs/GCE. So, the accumulation time of 150 s was maintained for further work.

3.7 Construction of calibration curve

In view of the enhanced electrochemical response of GEN at CDs/GCE, new analytical methods were proposed for its determination. For this, sensitive differential pulse voltammetric (DPV), square wave voltammetric (SWV) and adsorptive stripping differential pulse voltammetric (AdSDPV) methods were developed for the quantitative

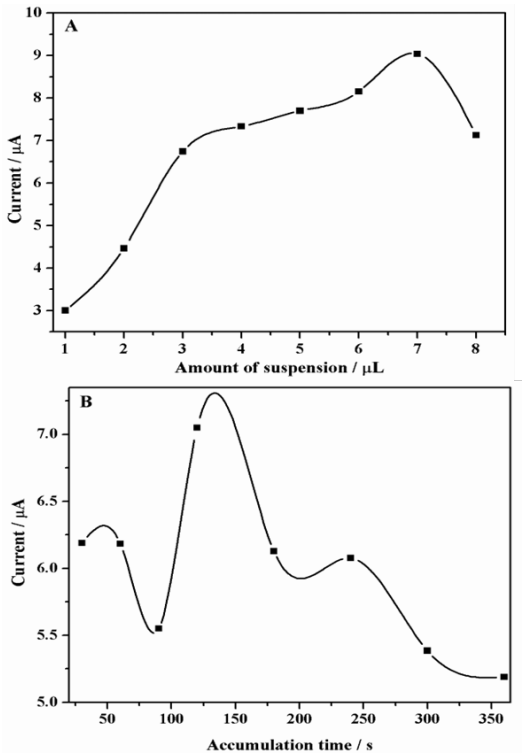

Figure 8: Dependence of peak current on the amount of CDs (A) and accumulation time (B)

determination of GEN in this work. Figure 9**A**, Figure 10**A** and Figure 11**A** displayed the DPV, SWV and AdSDPV responses for increased concentrations of GEN on CDs/GCE under optimized conditions. Linearity was observed between the peak current and concentration of GEN in the range of 0.5 - 30.01 μM, 0.1 - 54.16 μM and 1.0 - 62.5 μM for DPV, SWV and AdSDPV methods, respectively (Figure 9**B**, Figure 10**B** and Figure 11 **B)**. The corresponding regression equations are shown below:

$Ip/\mu A = 0.35\ [GEN] + 9 \times 10^{-9}$, $R^2 = 0.994\ (For\ DPV\ method)$

$Ip/\mu A = 0.46\ [GEN] + 4 \times 10^{-9}$, $R^2 = 0.988\ (For\ SWV\ method)$

$Ip/\mu A = 0.043\ [GEN] + 3 \times 10^{-9}$, $R^2 = 0.986\ (For\ AdSDPV\ method)$

The values of limit of detection (LOD) and limit of quantification (LOQ) for GEN were calculated from the calibration curve using the equations: LOD = 3s/m and LOQ = 10s/m, respectively, where s is the standard deviation calculated from intercept and m is the slope of the calibration graph. The detection limit was calculated to be 0.061, 0.042, and 0.36 μM respectively for DPV, SWV and AdSDPV methods. Among these three methods SWV method showed improved sensitivity because of its contribution of charging current to the background current is quite lower than that for DPV and AdSDPV methods (Table 2). RSD values were evaluated for inter- and intra- day assay of GEN by the proposed method and the corresponding results are listed in Table 2. Low values of RSD highlighted the reproducibility of the results.

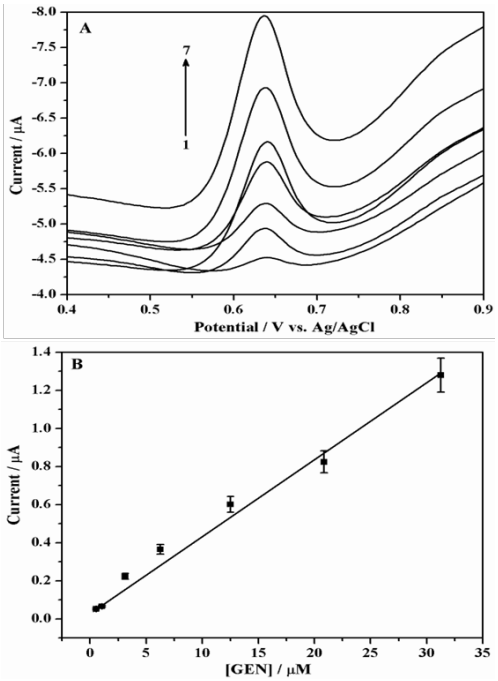

Figure 9: A) Differential pulse voltammograms for different concentrations of GEN [0.5 (1), 1.0 (2), 3.12 (3), 6.25 (4), 12.5 (5), 20.8 (6) and 31.01 (7) μM] at CDs/GCE in phosphate buffer of pH 3; B) Calibration plot

Table 2: Characteristics of the calibration plot for GEN

	DPV	SWV	AdS-DPV
Linearity range, μM	0.5 - 30.01	0.1 - 54.16	1.0 - 62.5
LOD, μM	0.061	0.042	0.36
LOQ, μM	0.21	0.14	0.81
Inter-day assay RSD* (%)	1.6	3.1	2.8
Intra-day assay RSD* (%)	2.04	2.43	3.05

* Average of 5 determinations

*3.8 **Reproducibility and stability of CDs/GCE***

The reproducibility and stability play an important role in monitoring the electrochemical process. Under optimized conditions, the CDs/GCE was used to determine 10 μM GEN for five times by SWV. Prior to each measurement, the electrode was reconstructed by drop casting CDs suspension on the clean surface of GCE. The fabricated sensor showed an almost same response and revealed reproducibility with RSD value of 3.12% for the determination of 5 μM GEN. In order to investigate the stability of the electrode, CDs/GCE

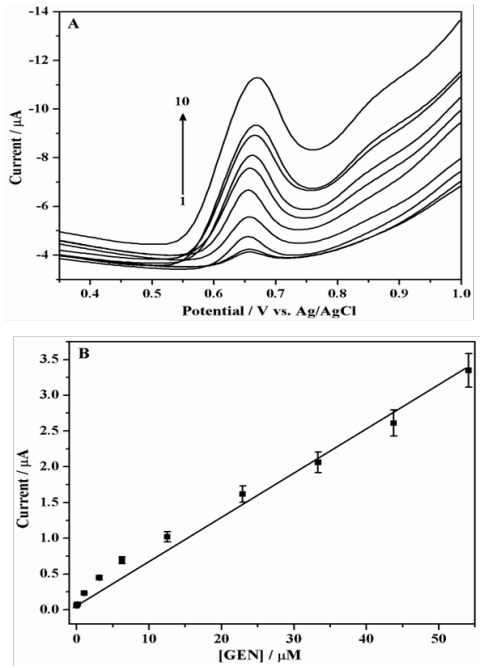

Figure 10: A) Square wave voltammograms for different concentrations of GEN [0.1 (1), 1 (2), 1.04 (3), 3.13 (4), 6.25 (5), 12.5 (6), 22.9 (7), 33.3 (8), 43.8 (9) and 54.16 (10) μM] at CDs/GCE in phosphate buffer of pH 3; B) Calibration plot

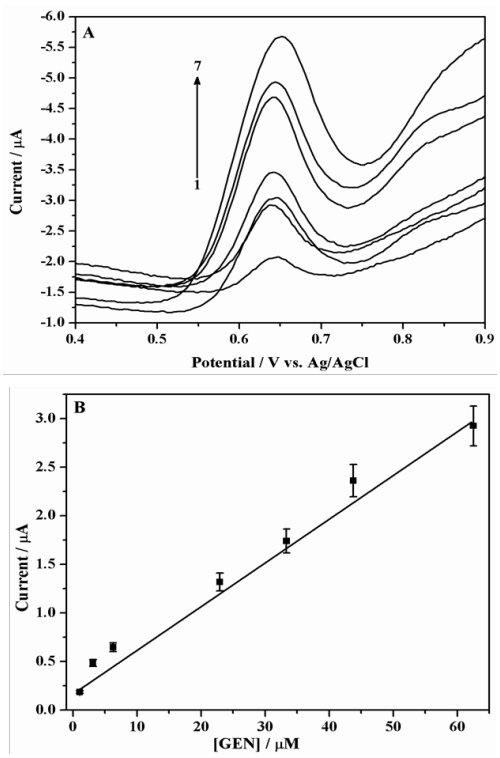

Figure 11: A) Adsorptive stripping differential pulse voltammograms for different concentrations of GEN [1.04 (1), 3.13 (2), 6.25 (3), 12.5 (4), 22.91 (5), 33.33 (6), 43.72 (7) and 62.5 (8) μM] at CDs/GCE in phosphate buffer of pH 3; B) Calibration plot

was stored at room temperature for more than 15 days. The peak current of GEN was decreased less than 4.5 % in SWV method compared with its initial current response. This illustrated that the proposed sensor material has excellent stability.

3.9 Interference studies

The selectivity of the proposed method was investigated by studying the effects of commonly occurring interferents viz., ascorbic acid, glucose, uric acid, starch, urea, acacia, lactose and thiourea on the electrochemical determination of 5 μM GEN. The tolerance limit was defined as the maximum concentration of the interfering component that caused an error less than 5 %. It was found that 155-fold of glucose, ~250-fold excess of lactose and ascorbic acid, 170-fold excess of starch, 230-fold excess of urea, 285-fold excess of uric acid and 107 fold excess of thiourea did not interfere in the determination of 5 μM GEN (Table 3). This suggests that the proposed electrode has excellent selectivity for the determination of GEN.

Table 3: Influence of interferents in the determination of 5 μM GEN using the proposed sensor by SWV method

Interfering sub-stance	Conc. of interfering substance (μg mL^{-1})	Fold	Recovery (%)	RSD*, %
Ascorbic acid	40	249	98.19	1.47
Glucose	25	155	98.89	1.08
Uric acid	15	285	97.50	2.16
Starch	20	171	97.11	2.42
Urea	14	230	98.39	2.05
Lactose	24	251	98.62	2.84
Thiourea	20	107	98.90	2.04

*Average of 5 determinations

3.10 Analysis of biological samples

The applicability of the proposed method was further demonstrated by analyzing GEN in human urine samples without any pre-treatment. The calibration graph was used to determine the concentration of GEN in urine samples. Table 4 summarizes the results of the analysis of urine samples. The recovery percentage was noticed in the range of 97.2 – 99.45 % and relative standard deviation (RSD) was in the range of 3-4%. These results indicated the good reproducibility of the electrode in real sample measurements indicating the feasibility of the electrode for practical applications.

3.11 Electrochemical behaviour of GEN in the presence of BSA

Cyclic and differential pulse voltammetric methods were used to investigate the interaction between GEN and BSA at CDs/GCE in phosphate buffer of pH 7. CV and DPVs

Table 4: Results of analysis of GEN in spiked human urine samples by SWV method

Amount of GEN added, μM	n	Amount found, μM	Average recovery (%)	RSD, %
2	5	1.95	97.50	2.46
4	5	3.98	99.50	1.51
6	5	5.88	98.00	2.12

of 20 μM GEN in the absence and presence of BSA at CDs/GCE are shown in Figure 12 **A** and **B**. Upon the addition of BSA to GEN, decrease in the peak current and negative shift in the peak potential was noticed. Further, no new peak was noticed in the presence of BSA. Two factors might be considered for the decrease in peak current. Firstly, the competitive adsorption between GEN and BSA on the surface of modified GCE and secondly, the formation of an electroinactive complex that decreased the concentration of GEN. The first factor could be excluded because the peak current of GEN did not disappear completely with increase in the concentration of BSA. Hence, decreased peak current without any changes in electrochemical parameter was considered as the indication of BSA-GEN electroinactive complex. Further, electrochemical kinetic parameters of GEN in the absence and presence of BSA were evaluated. The corresponding regression equations are shown below:

$E_{pa} = 0.034 \ln \upsilon + 0.78; R^2 = 0.989 (for\ free\ GEN)$

$E_{pa} = 0.035 \ln \upsilon + 0.18; R^2 = 0.993 (for\ GEN-BSA)$

From the slope of the plot of E_p vs. lnυ, the value of αn was calculated to be 0.76 and 0.73, for free GEN and GEN-BSA respectively. Further, from the intercept of the plot of E_p vs. lnυ, the values of electrochemical rate constant (k_s) in the absence and presence of BSA was calculated to be 1.07 and 1.06 s^{-1} respectively. These results revealed that there was no significant change in the electrochemical kinetics parameters for GEN in the absence and presence of BSA. So, we propose that the decrease in the electrochemical response of GEN upon the addition of BSA was due to the formation of an electrochemically inactive complex.

3.12 Determination of binding constant and binding number

According to the reported method [33], it is assumed that GEN interacts with BSA to form a single complex, BSA-mGEN according to the following reaction scheme:

$BSA + mGEN \leftrightarrow BSA-mGEN$

where m is the binding ratio. The equilibrium constant, β_s is deduced from the equation shown below:

$\log[\triangle I/(\triangle I_{max} - \triangle I)] = \log \beta_s + m \log[GEN]$

where ΔI is the difference in peak current of GEN in the presence and absence of BSA and ΔI_{max} is obtained when

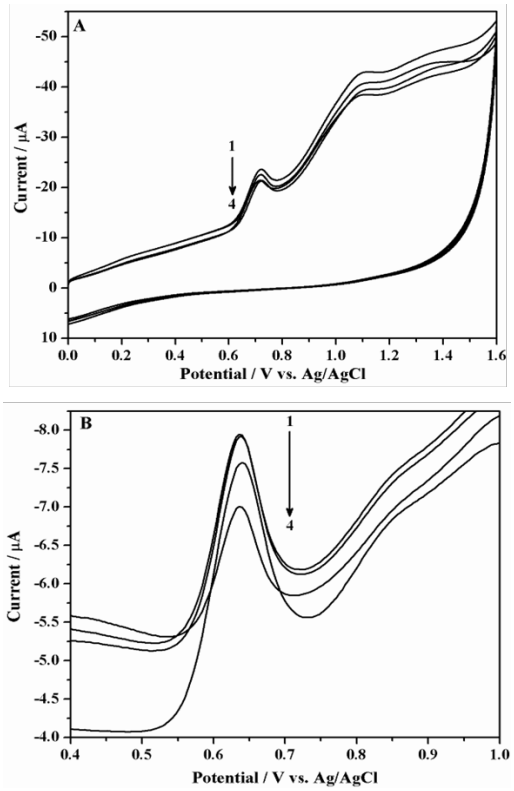

Figure 12: Cyclic (A) and differential pulse voltammograms (B) of 20 μM GEN (1) in the presence of increasing concentrations of BSA [5 (2), 10 (3) and 15 μM (4), respectively] at CDs/GCE in phosphate buffer of pH 7

the concentration of GEN is extremely high. The values of β_s and m were obtained from the slope and intercept of the plot of log[ΔI/(ΔI_{max} -ΔI)] vs. log [GEN], and the values were found to be 1.04 and 1.13 x 10^4 M^{-1}, respectively. This indicated that one molecule of GEN was bound to one molecule of BSA and formed a stable 1:1 complex, BSA-GEN.

3.13 Interaction of GEN with BSA-CDs/GCE

The immobilization of BSA on the electrode surface is in many ways the crucial aspect to develop a biosensor to monitor the biomolecule since it dictates the accessibility of BSA to biomolecule in solution. By considering this fact, we have carried out the interaction studies at BSA-CDs/GCE that was prepared by immobilization technique. Cyclic voltammograms of 10 μM GEN at CDs/GCE and BSA-CDs/GCE in the potential range of 0 – 1.6 V were recorded. Oxidation peak (a_1) potential was noticed to be shifted towards the negative value at BSA-CDs/GCE (Figure 13). The binding parameters are shown in **table 5**. This suggested the interaction between GEN and BSA to be through non-hydrophobic forces.

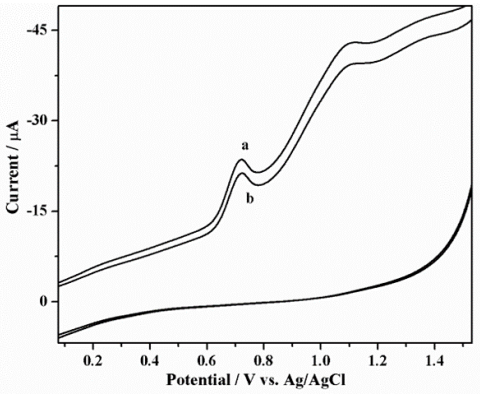

Figure 13: Cyclic voltammograms of 10 μM GEN at CDs/GCE (a) and BSA modified CDs/GCE (b) in phosphate buffer of pH 7

4 CONCLUSIONS

The present work describes the modification of GCE with CDs. The construction of CDs/GCE is simple, cheap, and environmentally friendly. The modified GCE showed excellent performance in the electrochemical determination of GEN. The modification of GCE decreased the charge transfer resistance and increased the analyte signal intensity. This electrochemical sensor was successfully utilized for the determination of GEN. Further, the developed electrochemical sensor showed excellent stability and sensitivity. The developed SWV method has a lower detection limit and provided good stability and sensitivity in the determination of GEN.

ACKNOWLEDGMENTS

The authors thank the University Grant Commission, New Delhi, for providing the financial support to carry out this work.

REFERENCES

1) S. P. Murphy and S. I. Barr, Challenges in using the dietary reference intakes to plan diets for groups, *Nutrition Reviews*, 63, *8*, 267 (2005)URL https://doi.org/10.1111/j.1753-4887.2005.tb00140.x.
2) S. Barnes, M. Kirk, and L. Coward, Isoflavones and their conjugates in soy foods: extraction conditions and analysis by HPLC-mass spectrometry, *Journal of Agricultural and Food Chemistry*, 42, *11*, 2466 (1994)URL https://pubs.acs.org/doi/10.1021/jf00047a019.
3) M. Naim, B. Gestetner, A. Bondi, and Y. Birk, Antioxidative and antihemolytic activities of soybean isoflavones, *Journal of Agricultural and Food Chemistry*, 24, *6*, 1174 (1976)URL https://pubs.acs.org/doi/10.1021/jf60208a029.
4) D. E. Pratt and P. M. Birac, Source of Antioxidant Activity of Soybeans and Soy Products, *Journal of Food Science*, 44, *6*, 1720 (1979)URL https://doi.org/10.1111/j.1365-2621.1979.tb09125.x.
5) L. Wu, J. B. L. Jr., and H. D. Dewald, Voltammetry and LCEC of isoflavones, *Electroanalysis*, 9, *10*, 796 (1997)URL https://doi.org/10.1002/elan.1140091013.
6) A. Franke and L. J. Custer, High-performance liquid chromatographic assay of isoflavonoids and coumestrol from human urine, *Journal of Chromatography B: Biomedical Sciences and Applications*, 662, *1*, 47 (1994)URL https://doi.org/10.1016/0378-4347(94)00390-4.
7) F. Luan, L. L. Tang, X. X. Chen, and H. T. Liu, Simultaneous Determination of Daidzein, Genistein and Formononetin in Coffee by Capillary Zone Electrophoresis, *Separations* , 4, *1*, 1 (2017)URL https://doi.org/10.3390/separations4010001.
8) I. da Costa César, F. C. Braga, C. D. Vianna-Soares, E. de Aguiar Nunan, G. A. Pianetti, and L. M. Moreira-Campos, Quantitation of genistein and genistin in soy dry extracts by UV-Visible spectrophotometric method, *Gérson Antônio Pianetti*, 31, *8*, 1933 (2008)URL https://doi.org/10.1590/S0100-40422008000800003.
9) X. Zhang, J. Zheng, and H. Gao, Electrochemical behavior of genistein and its polarographic determination in soybeans, *Analytical letters*, 34, *11*, 1901 (2001)URL https://doi.org/10.1081/AL-100106120.
10) O. M. Popa and V. C. Diculescu, Electrochemical behaviour of isoflavones genistein and biochanin A at a glassy carbon electrode, *Electroanalysis*, 25, *5*, 1201 (2013)URL https://doi.org/10.1002/elan.201200657.
11) J. Zhang and S. H. Yu, Carbon dots: large-scale synthesis, sensing and bioimaging, *Materials Today*, 19, *7*, 382 (2016)URL https://doi.org/10.1016/j.mattod.2015.11.008.
12) P.-C. Chen, Y. N. Chen, P. C. Hsu, C. C. Shih, and H. T. Chang, Photoluminescent organosilane-functionalized carbon dots as temperature probes, *Chemical Communications*, 49, *16*, 1639 (2013)URL https://doi.org/10.1039/C3CC38486A.
13) S. N. Baker and G. A. Baker, Luminescent carbon nanodots: emergent nanolights, *Angew. Chem., Int. Ed*, 49, *38*, 6726 (2010)URL https://doi.org/10.1002/anie.200906623.
14) Y. Dong, H. Pang, H. B. Yang, C. Guo, J. Shao, Y. Chi, C. M. Li, and T. Yu, Carbon-Based Dots Co-doped with Nitrogen and Sulfur for High Quantum Yield and Excitation-Independent Emission, *Angewandte Chemie International Edition*, 52, *30*, 7800 (2013)URL https://doi.org/10.1002/anie.201301114.
15) L. Bao, Z. L. Zhang, Z. Q. Tian, L. Zhang, C. Liu, Y. Lin, B. Qi, and D. W. Pang, Electrochemical tuning of luminescent carbon nanodots: from preparation to luminescence mechanism, *Advanced Materials*, 23, *48*, 5801 (2011)URL https://doi.org/10.1002/adma.201102866.
16) Y. P. Sun, B. Zhou, Y. Lin, W. Wang, K. A. S. Fernando, P. Pathak et al., Quantum-Sized Carbon Dots for Bright and Colorful Photoluminescence, *Journal of the American Chemical Society*, 128, *24*, 7756 (2006)URL https://pubs.acs.org/doi/10.1021/ja062677d.
17) X. Xu, R. Ray, Y. Gu, H. J. Ploehn, L. Gearheart, K. Raker, and W. A. Scrivens, Electrophoretic Analysis and Purification of Fluorescent Single-Walled Carbon Nanotube Fragments, *Journal of the American Chemical Society*, 126, *40*, 12736 (2004)URL https://doi.org/10.1021/ja040082h.
18) H. Li, X. He, Y. Liu, H. Huang, S. Lian, S.-T. Lee, and Z. Kang, One-step ultrasonic synthesis of water-soluble carbon nanoparticles with excellent photoluminescent properties Carbon, *Carbon*, 49, *2*, 605 (2011)URL https://doi.org/10.1016/j.carbon.2010.10.004.
19) B. Zhang, C. Liu, and Y. Liu, A Novel One-Step Approach to Synthesize Fluorescent Carbon NanoparticlesEur, *European Journal of Inorganic Chemistry*, 2010, *28*, 4411 (2010)URL https://doi.org/10.1002/ejic.201000622.
20) A. B. Bourlinos, A. Stassinopoulos, D. Anglos, R. Zboril, M. Karakassides, and E. P. Giannelis, Surface functionalized carbogenic quantum dots, *Small*, 4, *4*, 455 (2008)URL https://doi.org/10.1002/smll.200700578.
21) D. Pan, J. Zhang, Z. Li, C. Wu, X. Yan, and M. Wu, Observation of pH-, solvent-, spin-, and excitation-dependent blue photoluminescence from carbon nanoparticles, *Chemical Communications*, 46, *21*, 3681 (2010)URL https://doi.org/10.1039/C000114G.
22) R. Zhang and W. Chen, Nitrogen-doped carbon quantum dots: facile synthesis and application as a turn-off fluorescent probe for detection of Hg2+ ions, *Biosensors and Bioelectronics*, 55, 83 (2014)URL https://doi.org/10.1016/j.bios.2013.11.074.
23) X. Zhai, P. Zhang, C. Liu, T. Bai, W. Li, L. Dai, and W. Liu, Highly luminescent carbon nanodots by microwave-assisted pyrolysis, *Chemical Communications*, 48, *64*, 7955 (2012)URL https://doi.org/10.1039/C2CC33869F.
24) J. Zhang, W. Shen, D. Pan, Z. Zhang, Y. Fang, and M. Wu, Controlled synthesis of green and blue luminescent carbon nanoparticles with high yields by the carbonization of sucrose, *New Journal of Chemistry*, 34, *4*, 591 (2010)URL https://doi.org/10.1039/B9NJ00662A.

25) J. P. Doweiko and D. J. Nompleggi, Role of albumin in human physiology and pathophysiology, *Journal of Parenteral and Enteral Nutrition*, 15, *4*, 476 (1991)URL https://doi.org/10.1177/0148607191015004476.
26) J. P. Nicholson, M. R. Wolmarans, and G. R. Park, The role of albumin in critical illness, *BJA: British Journal of Anaesthesia*, 85, *4*, 599 (2000)URL https://doi.org/10.1093/bja/85.4.599.
27) J. R. Simard, P. A. Zunszain, C. E. Ha, J. S. Yang, N. V. Bhagavan, I. Petitpas, S. Curry, and J. A. Hamilton, Locating high-affinity fatty acid-binding sites on albumin by x-ray crystallography and NMR spectroscopy, *Proceedings of the National Academy of Sciences of the United States of America*, 102, *50*, 17958 (2005)URL https://doi.org/10.1073/pnas.0506440102.
28) K. Yamasaki, V. T. G. Chuang, T. Maruyama, and M. Otagiri, Albumin–drug interaction and its clinical implication, *Biochimica et Biophysica Acta (BBA) - General Subjects*, 1830, *12*, 5435 (2013)URL https://dx.doi.org/10.1016/j.bbagen.2013.05.005.
29) C. Bertucci and E. Domenici, Reversible and Covalent Binding of Drugs to Human Serum Albumin: Methodological Approaches and Physiological Relevance, *Current Medicinal Chemistry*, 9, *15*, 1463 (2002)URL https://dx.doi.org/10.2174/0929867023369673.
30) D. Sleep, J. Cameron, and L. R. Evans, Albumin as a versatile platform for drug half-life extension, *Biochimica et Biophysica Acta (BBA) - General Subjects*, 1830, *12*, 5526 (2013)URL https://dx.doi.org/10.1016/j.bbagen.2013.04.023.
31) Z. Zhu, L. Shi, H. Feng, and H. S. Zhou, Single domain antibody coated gold nanoparticles as enhancer for Clostridium difficile toxin detection by electrochemical impedance immunosensors, *Bioelectrochemistry*, 101, 153 (2015)URL https://dx.doi.org/10.1016/j.bioelechem.2014.10.003.
32) S. N. Prashanth, N. L. Teradal, J. Seetharamappa, A. K. Satpati, and A. V. R. Reddy, Fabrification of electroreduced graphene oxide–bentonite sodium composite modified electrode and its sensing application for linezolid, *Electrochimica Acta*, 133, 49 (2014)URL https://doi.org/10.1016/j.electacta.2014.04.022.
33) H. Heli, N. Sattarahmady, A. Jabbari, A. A. Moosavi-Movahedi, G. H. Hakimelahi, and F.-Y. Tsai, Adsorption of human serum albumin onto glassy carbon surface – Applied to albumin-modified electrode: Mode of protein–ligand interactions, *Journal of Electroanalytical Chemistry*, 610, *1*, 67 (2007)URL https://dx.doi.org/10.1016/j.jelechem.2007.07.005.